13

093018

JOURNAL OF GEOPHYSICAL RESEARCH, VOL. 109, F02005, doi:10.1029/2003JF000067, 2004

Sediment sorting and transport by flash floods

Daniel V. Malmon
Department of Geological Sciences, University of California, Santa Barbara, California, USA

Steven L. Reneau
Environmental Geology and Spatial Analysis Group, Los Alamos National Laboratory, Los Alamos, New Mexico, USA

Thomas Dunne
Donald Bren School of Environmental Science and Management and Department of Geological Sciences, University of California, Santa Barbara, California, USA

Received 21 July 2003; revised 17 February 2004; accepted 2 March 2004; published 23 April 2004.

[1] Flash floods partition the sediment load of arid and semiarid watersheds into components that travel at different rates through the fluvial system and are deposited in characteristic settings. This paper examines sediment sorting and transport by flash floods within a small, sand-dominated alluvial valley in a semiarid environment, upper Los Alamos Canyon, New Mexico. Floods in the study area partition the sediment load into two distinct facies: a coarse-grained facies that travels near the channel bed and a fine-grained facies that travels in suspension. The particle size distributions of channel and floodplain deposits resemble the measured textures of the bed load and suspended load, respectively. Calculations predict that typical flows sort the load into the same two fractions observed in the field. Whereas the transport rate of the coarse fraction depends on flow transport capacity, transport of the fine fraction is controlled by its supply. The long-term discharge of both fractions is estimated by integrating instantaneous transport relationships over the probability distribution of flows. Over several decades the computed fluxes of the two fractions are approximately the same. Most of the load in both fractions is transported during small to moderate events that occur more than once per year. However, the two fractions are distinct because they are supplied by different sources, transported by different mechanisms, and stored in distinct locations in the valley floor. Sediment sorting by flash floods is an important mechanism in constructing floodplains and in determining the residence times of various particle size classes in alluvial valleys. *INDEX TERMS:* 1815 Hydrology: Erosion and sedimentation; 1821 Hydrology: Floods; 1824 Hydrology: Geomorphology (1625); 1860 Hydrology: Runoff and streamflow; *KEYWORDS:* flash floods, sediment sorting, sediment transport, ephemeral channels, geomorphology of southwestern United States

Citation: Malmon, D. V., S. L. Reneau, and T. Dunne (2004), Sediment sorting and transport by flash floods, *J. Geophys. Res.*, *109*, F02005, doi:10.1029/2003JF000067.

RECEIVED
JUL 25 2006
By AM

1. Introduction

[2] A large portion of the terrestrial surface is drained through ephemeral channels. Sediment evacuation from these landscapes is accomplished by discrete flash floods traveling over dry streambeds. Sediment transport rates and mechanisms during flash floods can differ significantly from those during flows in perennial streams. Compared with runoff in more humid environments, flash floods are characterized by rapid fluctuations in flow and downstream losses of discharge due to infiltration into the streambed [*Babcock and Cushing*, 1941; *Burkham*, 1970]. Mobilization of bed sediment in gravel-bed ephemeral channels is enhanced by the absence or poor development of pavements, which are more commonly found in perennial gravel bed streams [*Laronne and Reid*, 1993; *Reid and Laronne*, 1995; *Reid et al.*, 1998]. Rates of scour and fill in sand bed ephemeral channels are also large compared with those in humid environments [*Leopold et al.*, 1964]. Widespread surface erosion of sparsely vegetated hillslopes due to frequent infiltration-excess overland flow [*Graf*, 1987] can produce large quantities of sand- and silt-sized sediment [*Leopold et al.*, 1966]. Floods triggered by rainstorms over such landscapes often have extremely high suspended sediment concentrations compared with those in humid landscapes, even during moderate runoff events [*Beverage and Culbertson*, 1964].

[3] The fluvial processes that sort the sediment load by particle size strongly influence the composition of both the bed and the banks and therefore channel form and stability. Over longer timescales, these sorting mechanisms deter-

Copyright 2004 by the American Geophysical Union.
0148-0227/04/2003JF000067$09.00

14471

mine the textures of fluvial deposits in subhumid landscapes and may contribute to the widely cited but poorly understood cycles of deposition and erosion that have occurred in valleys in the southwestern United States [*Schumm and Hadley*, 1957]. The size partitioning of sediment within valleys also determines where and over what timescale eroded material will remain in alluvial storage [*Malmon et al.*, 2003], making it an important process that decouples upland erosion from downstream sediment delivery.

[4] Much of the pollutant and nutrient load of rivers is carried on sediment [*Salomons and Forstner*, 1984; *Graf*, 1987, 1994, 1996]. In arid and semiarid environments the redistribution of this material by flash floods is a primary control on the fate of these constituents. Sediment-borne pollutants tend to concentrate on finer particles [*Purtymun et al.*, 1966; *Levinson*, 1980; *Graf*, 1987], which travel in suspension and can enter the floodplain. Sediment sorting causes contaminated sediment to accumulate in floodplains, which generally have long particle residence times compared with sediment stored within the channel margins. A mechanistic understanding of sediment partitioning by flash floods is therefore necessary for developing realistic models of contaminant transport in semiarid landscapes.

[5] The global database on sediment transport by flash floods is gradually increasing as a result of field investigations in the southwestern United States [*Renard and Laursen*, 1975], southern Israel [*Gerson*, 1977; *Lekach and Schick*, 1982; *Schick et al.*, 1987; *Laronne and Reid*, 1993], Kenya [*Frostick et al.*, 1983; *Reid and Frostick*, 1987; *Sutherland and Bryan*, 1989], Spain [*Martin-Vide et al.*, 1999], and India [*Sharma et al.*, 1984]. These studies have provided data on the rates and particle size distributions of sediment in transport and have led to some generalizations about sediment dynamics during flash floods. A primary conclusion drawn from these data is that instantaneous transport rates during flash floods are generally greater than they would be for similar discharges or shear stresses in perennial streams. The higher transport rates are presumably related to greater rates of sediment supply, both from sparsely vegetated hillslopes and from unarmored channel beds. Analyses of these data have been limited to developing empirical relationships between transport rates and various parameters related to discharge or rainfall characteristics, but the physical mechanisms of sediment transport and their relationship to the driving hydrology have not been examined in detail. Understanding the transport mechanisms operating for particles of different size is central to the sorting process, which determines where and in what quantity the sediment load can be stored.

[6] In this paper we document fluvial sediment transport and sorting by flash floods over a range of timescales (from hours to decades) in a small alluvial valley in New Mexico. The valley has a sand-dominated, ephemeral channel and a narrow floodplain. Valleys with similar features are frequently encountered in semiarid environments, particularly in the southwestern United States. Frequent flash floods occur during the summer "monsoon" season. Sediment is also transported during a relatively low snowmelt runoff period lasting up to several months. Data from flash floods in upper Los Alamos Canyon, New Mexico, are used to identify the mechanisms and quantify the rates of sediment transport during small to moderate runoff events. A simplified model of vertical sediment concentration profiles for a range of size classes (using the Rouse equation) predicts that sediment should be sorted by particle size into two discrete populations. This prediction is confirmed with an extensive sedimentological data set that exists for the study area [*Reneau et al.*, 1998]. Finally, instantaneous transport relationships are extrapolated over time using a synthetic population of hydrographs to compute the long-term average fluxes of both sediment fractions from the watershed and to examine its frequency and magnitude attributes.

2. Field Area

2.1. Geology and Geomorphology

[7] Upper Los Alamos (ULA) Canyon (Figure 1) drains a watershed composed primarily of volcanic rocks. The watershed heads in the eastern Jemez Mountains, and the upper basin is underlain by dacitic lavas of the Mio-Pliocene Tschicoma Formation [*Smith et al.*, 1970]. The lower portion of the watershed drains mesas and canyon walls of the Pajarito Plateau, underlain largely by Pleistocene ignimbrites of the Bandelier Tuff. Soils developed on the Bandelier Tuff are typically sandy and cobbly loams dominated by silt- and sand-sized particles [*Nyhan et al.*, 1978]. Nearly all the runoff and sediment load under normal circumstances is derived from areas underlain by the Bandelier Tuff [e.g., *Shaull et al.*, 2003].

[8] This study focuses on a 5.3 km reach of valley floor between two major tributaries, DP and Pueblo Canyons (Figures 1 and 2), within the Los Alamos National Laboratory (LANL). The drainage area of ULA Canyon above Pueblo Canyon is 28 km^2, and the total relief is 1260 m. ULA Canyon is one of approximately 20 subparallel canyons that dissect the Pajarito Plateau and drain into the Rio Grande. The average channel slope in the study area is 0.02, and there are no major downstream changes in gradient along the study reach between DP and Pueblo Canyons (Figure 2).

[9] The bottoms of canyons draining the Pajarito Plateau are mostly alluvial, although bedrock reaches prevail in parts of lower-order tributaries [e.g., *Katzman et al.*, 1999] and in some downstream reaches flowing through pre-Bandelier basalts. The floodplain along the study reach is narrow, confined by the canyon walls and at least one large bouldery unit deposited by a large debris flow or flood event dated at circa 1300–1650 A.D. [*Reneau and McDonald*, 1996]. The significance of this unit in the current study is in setting the boundary conditions, affecting the width and slope of the valley; its importance as a sediment source is limited due to the high resistance to entrainment of the boulders. The spatial distribution of LANL-related radionuclides indicates that the width of the valley floor that has been active since 1942 averages <10 m [*Reneau et al.*, 1998]. Channel width varies from 1 to >3 m, averaging 1.9 m, and bank height varies from 0.2 to 3 m, averaging 0.7 m [*Malmon*, 2002].

2.2. Climate and Runoff Generation

[10] Mean annual precipitation at the town of Los Alamos (Figure 1) is 46 cm yr^{-1} [*Bowen*, 1990]. About 60% of the precipitation occurs from June to October [*Malmon*, 2002], which includes the summer monsoon-like season.

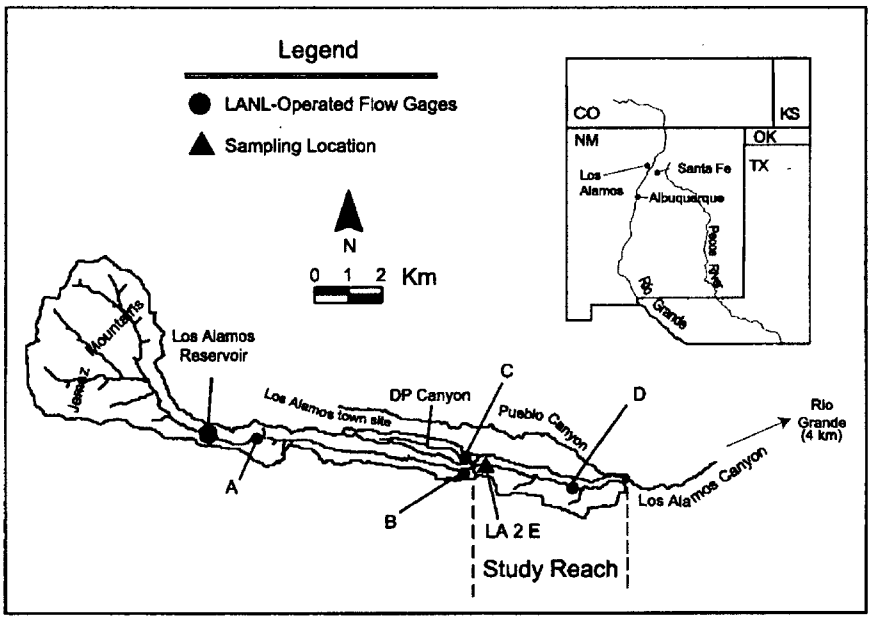

Figure 1. Map of upper Los Alamos Canyon. The study reach is the 5.3 km stretch of valley between DP Canyon and Pueblo Canyon.

Flash floods during these months are generated by convective thunderstorms and occasional frontal storms. Urbanization on the mesa top within the DP Canyon watershed (Figure 1) has increased the frequency and magnitude of flow in both DP and ULA Canyons since 1942, when the initial facilities housing LANL were built. Although a large portion of the watershed of ULA Canyon lies in the Jemez Mountains (Figure 1), under typical conditions, storm runoff is generated by rainfall over the sparsely vegetated ponderosa pine and piñon-juniper environments on the Pajarito Plateau [*Wilcox*, 1994; *Wilcox et al.*, 1997; *Newman et al.*, 1998] and over the urbanized areas [*Shaull et al.*, 2003].

[11] Spring snowmelt runoff lasts an average of 66 days (±38 days) at the downstream boundary of the study reach, based on 7 years of data compiled by *Purtymun et al.* [1990]. While the duration of snowmelt flow is longer than that of storm flow, it is not associated with the widespread erosion and rapid flow fluctuations that characterize storm runoff events. In general, snowmelt remains within the channel banks and carries little or no wash load. In this case the term "flash flood" refers to rainfall-generated storm runoff, which generally occurs during the summer monsoon season and occasionally following fall frontal rainstorms. Snowmelt is only considered with respect to long-term bed load transport, and its influence on the wash load flux is assumed to be minor.

2.3. Cerro Grande Fire, May 2000

[12] In May 2000 the Cerro Grande fire burned much of the eastern Jemez Mountains and western Pajarito Plateau, including 44% of the ULA Canyon watershed [*Burned Area Emergency Rehabiliatation Team*, 2000]. Most of the severely burned portions of the watershed lie above the Los Alamos Reservoir (Figure 1). Repeated surveys of the reservoir indicate that sediment yields from the burn area temporarily increased by more than two orders of magnitude [*Lavine et al.*, 2001]. However, the reservoir has buffered the influence of the fire on hydrology and sediment transport in the study reach considered in this paper.

[13] Burning can significantly influence the sediment yields of semiarid landscapes, both by increasing the supply of sediment from hillslopes and by increasing the amount of rainfall that becomes storm flow in channels. In watersheds impacted by the fire the supply of fine sediment has increased dramatically. However, even in the most severely

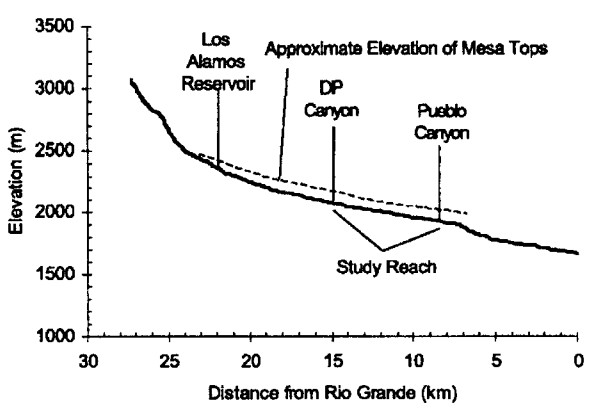

Figure 2. Upper Los Alamos Canyon longitudinal profile. The approximate relative elevation of the mesa tops is indicated with a dashed line. The longitudinal profile is derived from U.S. Geological Survey 1:24,000 topographic maps.

burned watersheds the basic mechanisms of sediment sorting that are the focus of this paper have continued to operate, though at elevated rates [*Malmon et al.*, 2002]. While the geomorphic effect of major perturbations such as wildfires is an important area of ongoing research, including locally [e.g., *Cannon et al.*, 2001; *Johansen et al.*, 2001; *Lavine et al.*, 2001; *Moody and Martin*, 2001; *Wilson et al.*, 2001; *Malmon et al.*, 2002], that topic is not the focus of this paper. Instead, the purpose is to document and quantify the mechanisms by which the incoming sediment load is sorted by floods in a typical small valley in a semiarid environment.

3. Methods

[14] This paper includes data from a variety of sources. We used data from eleven LANL-operated recording rain gauges [*Stone and Holt*, 1996] and four stream gauges (A–D, Figure 1) within or near the ULA Canyon watershed [*Shaull et al.*, 2003]. We intensively monitored runoff and sediment transport at a site in ULA Canyon just below the confluence with DP Canyon ("LA 2 E," Figure 1). All suspended and bed load data presented in this paper were collected following rainstorm events between June and October 1998 and 1999, prior to the Cerro Grande fire.

[15] Flood stage during sampling was estimated from two staff gauges read concurrently at site LA 2 E, ~100 m downstream of the ULA-DP confluence (Figure 1). When personnel were not present during sampling, stage estimates were obtained from an automated pressure transducer installed 10 cm above the bed. Five crest stage gauges [*Harrelson et al.*, 1994] were also installed in the sampling reach to provide an independent check on peak flood stage and water surface slope during runoff events. Corresponding discharges were estimated using rating curves developed from channel cross sections and the Manning equation (assuming the channel roughness coefficient is 0.04, based on a compilation of velocity measurements during flash floods using current meters (D. Shaull, Los Alamos National Laboratory, unpublished data, 1999) and floats [*Malmon*, 2002]). Discharge estimates from these methods generally agreed with simultaneous discharges estimated above the ULA-DP confluence at the LANL-operated stream gauges B and C (Figure 1).

[16] Suspended sediment samples were collected during 10 floods at site LA 2 E. Most samples were collected using a manual depth-integrated (U.S. Geological Survey DH-48) sampler while wading in the flow. In addition, some samples were collected at LA 2 E using an automated pump sampler (ISCO brand) with a fixed intake port located roughly 15 cm above the bed (this value is approximate due to fluctuations in bed elevation). There was no significant difference in sediment concentration between 45 pairs of samples collected concurrently using the manual and automatic pump samplers (subject to a paired *t*-test with $\alpha = 0.05$).

[17] Bed load was measured at site LA 2 E using a Helley-Smith sampler [*Helley and Smith*, 1971] with a 7.5 × 7.5 cm intake port and a sample bag with a 0.25 mm mesh. Thus only medium sand and coarser particles were sampled; sediment finer than medium sand (<0.25 mm) is considered wash load on the basis of suspendibility calculations and particle size data, discussed in section 4. Although efforts were made to not to disturb the bed, Helley-Smith samplers tend to sink into sand bed channels during sampling, leading to possible overestimation of the bed load flux. The shallowness of the flow allowed close manual control on the sinking, but the magnitude of this uncertainty is unknown. Thus estimates of instantaneous bed load flux might best be considered maximum values.

[18] The relative simplicity of the measurement techniques and the rapidly changing flow and channel conditions create several other potential sources of measurement error. We consider the most important of these sources to be inaccuracies in our estimates of flow variables due to scour and fill of the channel bed. Although the crest stage gauges and transducers that we used to measure flow depth and water surface slope can measure the water surface to ~1 cm, scour and fill of the channel bed can lead to much larger uncertainties. Our primary measurement site at LA 2 E was chosen partly due to the apparent stability of the channel at that site; however, scour chains at the site indicated scour depths up to 15 cm (up to about 20% of flow depth) during the highest flows [*Malmon*, 2002]. We did not account for scour and fill in our estimates of flow depth because of uncertainties about the magnitude and timing of these changes. Thus any estimates that are based on flow depth (i.e., discharge, velocity, and shear stress) should be considered approximations.

4. Sediment Sorting by Flash Floods

4.1. Observations of Sediment Transport During Flash Floods

[19] Storm flow is produced by discrete rainfall events, mainly during summer and fall. Flash floods in the channels draining the Pajarito Plateau rise rapidly following the flood bore (Figure 3), often reaching peak discharge within the first 5 min of flow (Figure 4). A small flow event on 14 September 1999, for which there is a particularly good record of rainfall, flow, and suspended sediment concentrations, illustrates suspended sediment characteristics in a typical flood event. The temporal relationship between rainfall and runoff for this event is shown in Figure 4a. The peak discharge was 0.6 $m^3 s^{-1}$, a discharge that occurs more than once per year on average [*Malmon*, 2002]. Mean depth at peak flow was 0.25 m. While the concentration of coarse sediment in suspension tends to respond to changes in discharge, the concentration of fine sediment is more strongly correlated with time. Fine sediment concentrations were highest near the flood bore and decreased rapidly, particularly for the finer portion of the load (Figure 4b). A second discharge peak, generated by a second burst of rainfall (Figure 4a), was not associated with a major increase in suspended sediment concentration comparable with the values attained during the initial flood peak (Figure 4b). A rapid initial decrease in fine sediment concentration following the passage of the flood bore is a characteristic common to every flood that has been sampled in the area, both before and since the Cerro Grande fire [*Dale*, 1996; *Malmon*, 2002; *Malmon et al.*, 2002]. This pattern has also been observed in flash floods elsewhere [e.g., *Sharma et al.*, 1984; *Reid and Frostick*, 1987; *Dunkerley and Brown*, 1999].

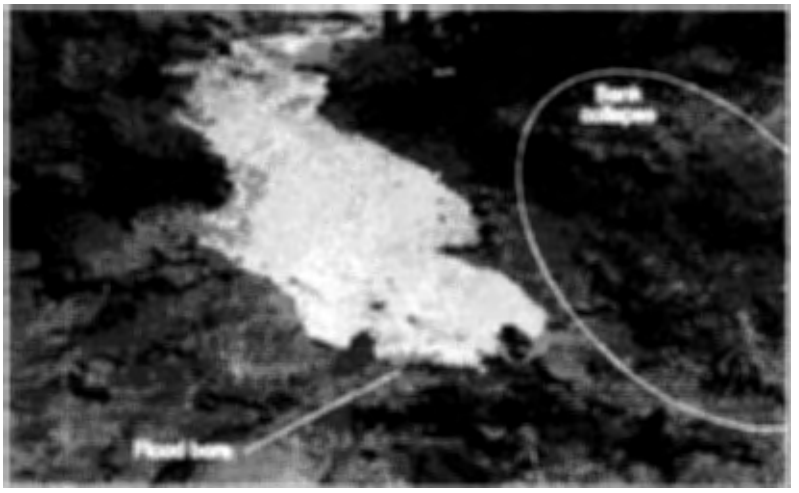

Figure 3. Photograph of a small flood bore, upper Los Alamos Canyon, summer 1999. Fine sediment is supplied to the flood partly by small bank collapses (lower right) prior to the arrival of the flood bore.

[20] The simplest interpretation of these data is that fine sediment transport in ULA Canyon is limited by supply, not flow transport capacity, and that more fine sediment is available for transport during the earliest part of the flow. Several sources of this material have been noted in the field.

[21] 1. The increased supply of fine sediment near the flood bore is partly the result of bank collapse, which can occur after the flood, leaving fine sediment on the bed that is available to the next flood bore (Figure 3). This is consistent with the observation of *Leopold and Miller* [1956, p. 4] that bank caving following flood recession is an important part of the sediment load of small ephemeral channels.

[22] 2. Field observations indicate that additional fine sediment can also be made available to flood bores by bioturbation of soil on the banks during intervals between flow events; this process also likely contributes sediment to overland flow on hillslopes. The importance of bioturbation depends largely on the duration between storm events and therefore may contribute to seasonal variations in sediment supply; however, our data are not sufficient to substantiate this hypothesis.

[23] 3. Elevated transport rates near the flood bore may also come from remobilization of fines in the channel bed, which are present due to the infiltration of previous floods. *Renard and Laursen* [1975] also noted hysteresis in sediment concentration during four flash floods in Walnut Gulch and attributed it to the presence in the bed of residual fine sediment deposited during the waning stages of preceding flows. Samples of the bed material from the active channel in ULA Canyon contained about 6% fines [*Reneau et al.*, 1998]. In nearby Pueblo Canyon, following the Cerro Grande fire (which supplied a large quantity of fine sediment to the channel), samples of the active bed material typically contain between 10 and 20% fines (D. Katzman, Los Alamos National Laboratory, personal communication, 2004).

[24] In ULA Canyon, transport of fine sediment is controlled by its supply from the channel bed, banks, and hillslopes, although the relative importance of the three sources has not yet been established. Each of these tends to deliver more sediment to the early part of the flood than to the long falling limb, leading to fine sediment concentrations that decrease with time after the passage of the flood bore.

4.2. Mechanisms of Sediment Transport

[25] In order to better understand the physical mechanisms of sediment transport during flash floods, approximate concentration profiles were computed for each depth-integrated sample using the Rouse equation [*Rouse*, 1937]:

$$C_i(z) = A(i)\left(\frac{H-z}{z}\right)^{\frac{w_i^*}{\kappa u_*}}, \qquad (1)$$

where $C_i(z)$ is the concentration of particle size class i at a height z above the channel bed, H is flow depth, w_i^* is the settling velocity for particle size class i (computed using the relationships from *Dietrich* [1982]), u_* is shear velocity (approximated as $\sqrt{gHS}$, where g is gravity and S is water surface slope), κ is the von Kármán constant (0.4), β is the ratio of momentum diffusion to sediment diffusion (assumed here to be 1), and $A(i)$ depends on the concentration of i at some reference elevation near the channel bed. We chose the reference elevation to be 2 mm (about $2 \times D_{50}$). We calculated the near-bed concentration of each size class using the measured depth-integrated concentration above 7.5 cm by rearranging equation (1) and solving for the value of $A(i)$ that produced a vertical concentration profile that was consistent with the measured depth-integrated concentration. The computed concentration profiles for a single depth-integrated sample (sample 321, the first sample collected following the passage of the 14 September 1999 flood bore) are shown in Figure 5. The Rouse model predicts that coarse sand and coarser sediment (i.e., particles larger than 0.5 mm diameter) concentrate near the bed, while the fine sand, silt, and clay (particles smaller than 0.25 mm) are relatively well mixed in the flow. Medium sand (0.25–0.5 mm) is moderately well mixed,

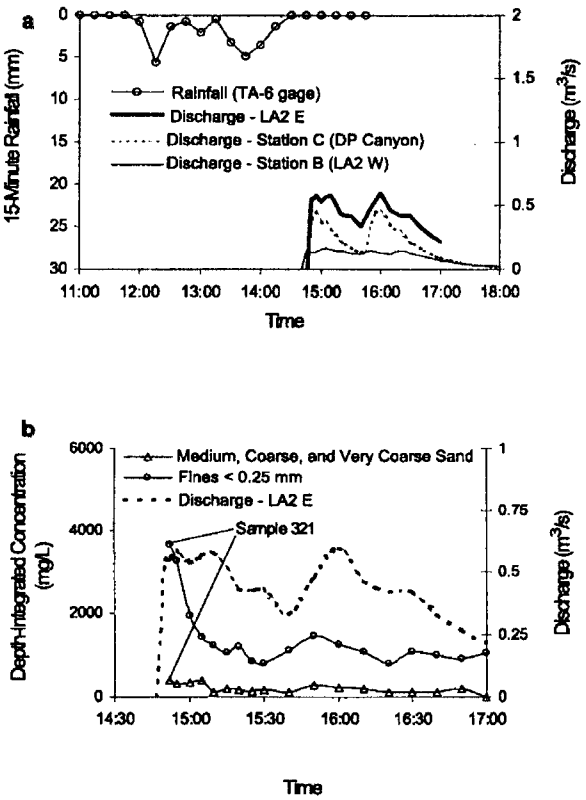

Figure 4. Rainfall, runoff, and sediment concentration at site LA 2 E during the 14 September 1999 runoff event. (a) Rainfall hyetograph and discharge hydrographs. Flow above the confluence of the ULA (gauge B, Figure 1) and DP (gauge C, Figure 1) Canyons was measured at LANL-operated stream gauges and below the confluence (LA 2 E) from manual staff gauge readings during flow. Rainfall data are from the recording rain gauge at TA-6, on a mesa south of the upper Los Alamos Canyon watershed. (b) Hydrograph and suspended sediment concentration during flood, measured using a depth-integrated (DH-48) sampler while wading in flow. The peak flow depth was ~0.25 m at the measuring site, ~0.15 m below the bank full depth. Sample 321, for which computed vertical sediment concentration profiles are shown in Figure 5, is labeled.

according to the model. The concentration profiles illustrated in Figure 5 are characteristic of profiles that would be computed for the range of hydraulic conditions typical of flash floods in small, sand-dominated ephemeral channels, i.e., flow depths of <1 m and energy gradients near 2%. Large, infrequent events may drive coarser sediment higher into the water column, but for most flows the calculations suggest that the suspended load should contain mostly fine sand and finer sediment.

[26] There are many limitations to this simple method for computing the sediment concentration profile. Equation (1) ignores a number of factors that may influence the concentration profile, including the effects of density stratification, of bed forms, and of interactions between multiple particle size classes [*McLean*, 1991]. These factors probably influence the concentration profiles locally, given the typically low flow depths and high suspended sediment concentrations (although bed forms are not widely observed). However, the purpose of these calculations is to aid in interpreting our field data, not to make highly accurate predictions of the vertical sediment concentration profile. Furthermore, density stratification would tend to reduce upward mixing for coarse sediment, and interactions between multiple size classes would tend to inhibit the settling of fines [*McLean*, 1991]. Thus including these factors in the model would predict even stronger sorting of coarse and fine sediment during floods.

4.3. Relationship Between Transport Mechanics and Sedimentology of Valley Floor Deposits

[27] Two distinct types of recent sedimentary deposits can be easily distinguished in the field on the basis of texture and spatial relationships [*Reneau et al.*, 1998]. Coarse deposits form the bed of the active channel and underlie or are locally interstratified with fine-grained deposits below adjacent floodplains (Figure 6). The coarser layers underlying the floodplain in Figure 6 are generally similar in texture to the active channel sediments, though they do contain a slightly higher proportion of fine-grained sediment, which we interpret to reflect postdepositional bioturbation.

[28] The particle size distributions of the active channel and floodplain deposits (Figure 7a) resemble those of the bed load and suspended load, respectively (Figure 7b). Both the bed load and the bed material are dominated by particles larger than 0.25 mm, and the suspended load and the floodplain deposits are mostly finer than 0.5 mm; particles between 0.25 and 0.5 mm (i.e., medium sand) are found in both sediment facies. There is some overlap in the particle size distributions that can be explained by processes ob-

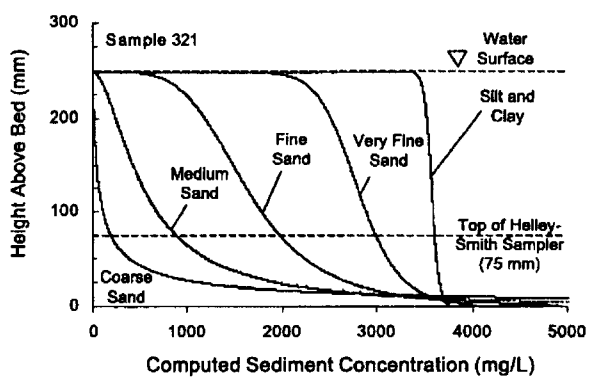

Figure 5. Computed vertical sediment concentration profiles for a sample collected near the 14 September 1999 flood bore at LA 2 E (sample 321, labeled in Figure 4b). See text for an explanation of the calculations. According to the theory, fine sand and smaller particles are relatively well mixed and travel primarily in suspension, even during a relatively small event. Coarse and very coarse sand concentrate near the bed (gravel was not found in any of the depth-integrated samples). Medium sand is moderately well mixed.

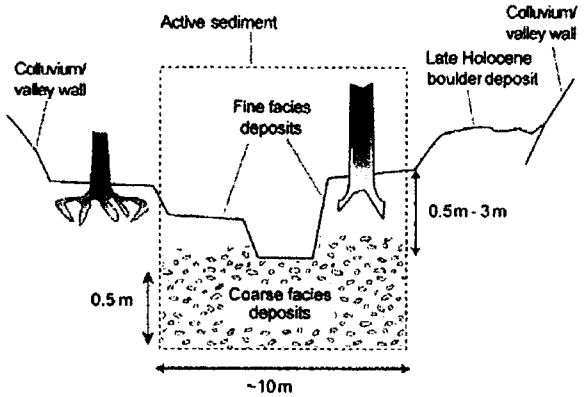

Figure 6. Schematic cross section of the valley floor depicting the spatial distribution of coarse and fine sediment in the active portion of the valley floor.

served in the field, including vertical mixing of floodplains as a result of bioturbation, suspended sediment infiltration into the bed, and flow events larger than the events we sampled. However, Figure 7 demonstrates that there are two distinct populations of recent fluvial deposits in the valley reach.

4.4. Conceptual Model of Sediment Sorting and Valley Formation

[29] The computed sediment concentration profiles (Figure 5) and the measured particle size distributions of the sediment load and the valley floor deposits (Figure 7) lead to a conceptual model of valley formation, in which the incoming sediment load is partitioned into two distinct components: a fine fraction that can be exchanged with the floodplain and a coarse fraction that can be exchanged with the channel bed. The transport rate of the fine fraction is supply controlled, while transport of the coarse fraction is controlled by flow transport capacity.

[30] In the rest of this paper the sediment load is divided into two distinct populations called fine sediment and coarse sediment based on the nature of the deposits with which they can be exchanged. We define these terms as follows (see Figure 8 for a definition sketch). Coarse sediment is that fraction of the load that is likely to be stored in the channel bed: gravel, very coarse sand, coarse sand, and the portion of the medium sand traveling near the bed. Fine sediment consists of the wash load (particles smaller than medium sand) plus the portion of the medium sand that travels high enough in the flow to enter the floodplain. Medium sand is partitioned among the two fractions according to the ratio of the sediment flux that travels above and below the minimum height of the floodplain surface, which is ~0.2 m in the study reach (based on measurements by *Malmon* [2002]).

[31] There is an additional component of the bed load, consisting of cobbles and larger particles that were not sampled, that is not included in this analysis, except to the extent that it affects the roughness of the channel. Although it is difficult to quantify the impact of this exclusion, it is probably small because these particles are believed to travel much more slowly and less frequently than the sand. This interpretation is based on the absence of cobbles and larger particles that appeared to be in motion while wading in moderate flows in ULA Canyon.

5. Sediment Transport Rates

[32] Each of the modes of sediment transport is quantified in this section using measurements of instantaneous sediment transport by flash floods in the study reach. The conceptual model developed in section 4.4 distinguishes two separate components of the sediment load: a coarse facies, which includes all the bed load and a portion of the bed material suspended load, and a fine facies, which includes all the wash load and the remainder of the bed material suspended load (Figure 8). The bed material suspended load (medium sand) was partitioned between the two components of the sediment load using the following rule: the portion of the medium sand traveling above the

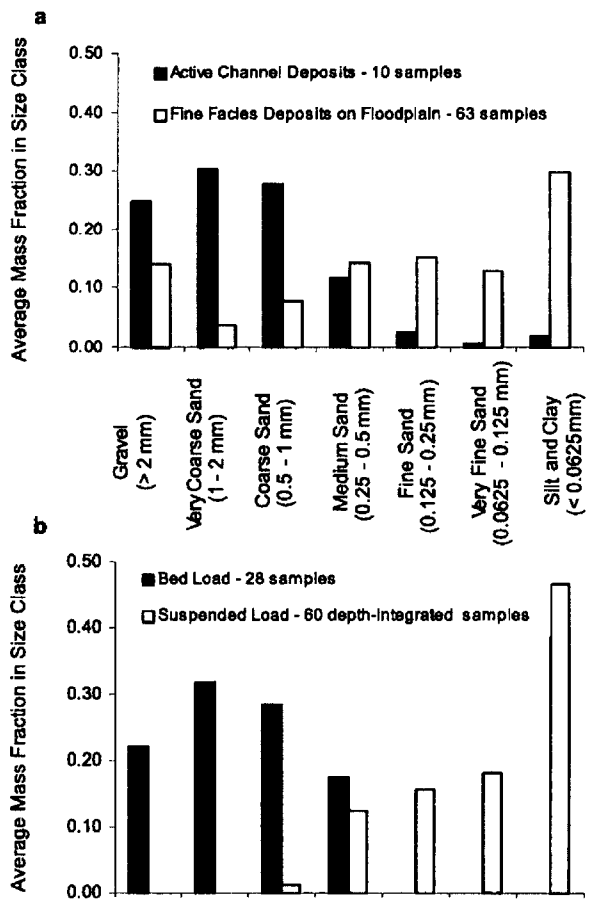

Figure 7. Average particle size distributions for (a) active channel and floodplain deposits in the valley floor (based on data presented by *Reneau et al.* [1998]) and for (b) bed load and suspended sediment samples collected during flood events (summers of 1998–1999). The mesh diameter on the bed load sampler is 0.25 mm, equivalent to the size break between medium and fine sand.

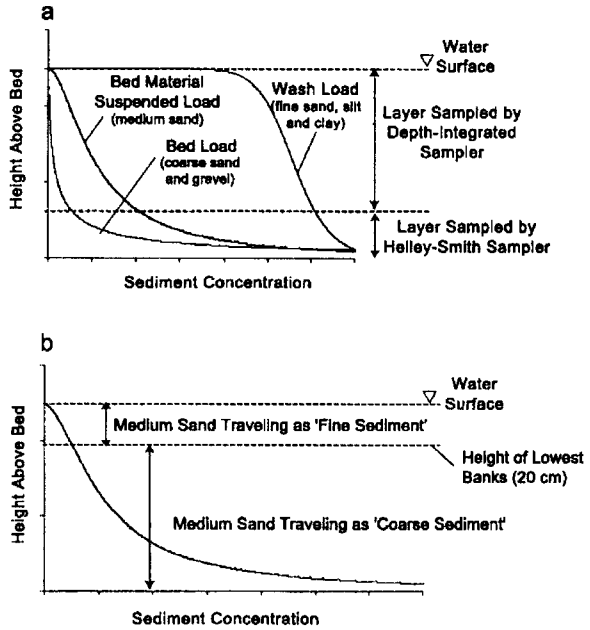

Figure 8. Definition sketch of sediment transport mechanisms in the study area, depicting typical sediment concentration profiles. (a) Distinction between bed load, wash load, and bed material suspended load based on typical concentration profiles. (b) Computational method of partitioning medium sand, which is found in both the channel bed and the floodplain, among fluxes of coarse and fine sediment facies. Medium sand traveling above the lowest bank height (20 cm) can be deposited on the floodplain and is counted with the fine portion of the load, while medium sand traveling below this height is included with the coarse facies.

height of the lowest banks (with the potential of depositing in the floodplain) is considered with the fine fraction, and the portion of medium sand traveling below the lowest banks is counted as part of the coarse fraction (Figure 8b).

[33] In this section, instantaneous transport relationships for each fraction of the sediment load are developed based on data from samples collected during flash floods. These models are then extrapolated in time by applying them to the probability distribution of flow in ULA Canyon.

5.1. Instantaneous Rates of Sediment Transport

5.1.1. Coarse Fraction

[34] As defined in section 5, the coarse fraction consists of the bed load (particles larger than 0.5 mm diameter) and part of the bed material suspended load (medium sand particles between 0.25 and 0.5 mm). Bed load is the portion of the sediment load that travels by rolling, sliding, or saltating near the bed. In typical floods, this includes particles larger than ~0.5 mm (coarse sand and gravel); this material is mostly contained in the bottom layer of flow sampled by the Helley-Smith sampler (Figure 8a). Because the source of this material is the channel bed, the instantaneous bed load transport rate depends primarily on flow and sediment characteristics rather than on the supply from outside the channel. We found that the bed load flux at the sampling site increases approximately with the square of shear stress (Figure 9a):

$$q_{bl} = 0.06\tau_*^{2.0}, \tag{2}$$

where q_{bl} is the instantaneous flux of particles coarser than 0.5 mm per unit width and τ_* is dimensionless bed shear stress, defined as

$$\tau_* = \frac{\tau_b}{(\rho_s - \rho)D} \simeq \left(\frac{\rho g h S}{(\rho_s - \rho)D}\right), \tag{3}$$

where ρ_s and ρ are the density of sediment and water, respectively, D is particle diameter (assumed to be equal to

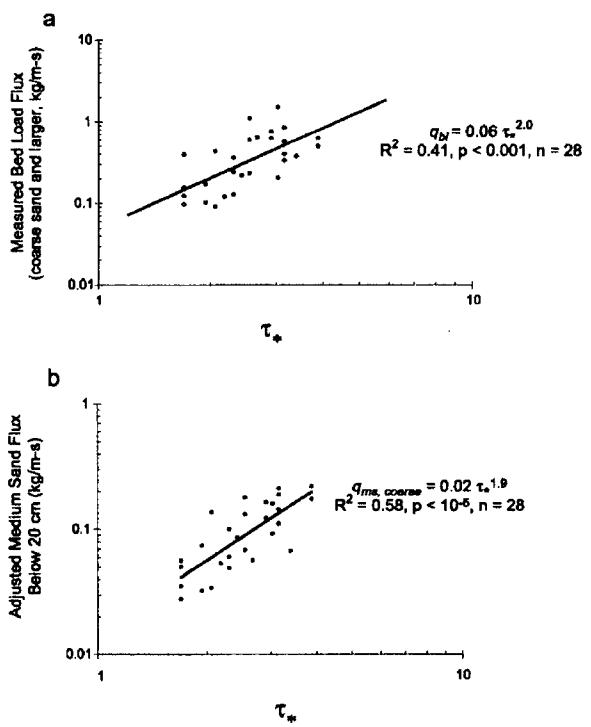

Figure 9. Instantaneous transport rates of the coarse sediment fraction. (a) Bed load, consisting of particles larger than 0.5 mm diameter (coarse sand and coarser). We assume that the entire bed load is measured with the Helley-Smith sampler, which samples the lowest 7.5 cm of flow. (b) Suspended bed material load (medium sand, 0.25–0.5 mm) traveling below the height of the lowest banks (20 cm). Fluxes in Figure 9b are based on Helley-Smith measurements and are adjusted to account for the nonsampled increment of flux between 7.5 and 20 cm in the flow using the Rouse equation and assuming a logarithmic water velocity profile. Coefficients in both regression equations were adjusted to account for transformation bias using a nonparametric correction factor [*Duan*, 1983]. The instantaneous flux of coarse sediment equals the sum of the bed load and the suspended bed material load traveling below the height of the banks (see Figure 8 for a definition sketch).

1 mm, the median diameter of the bed material), S is the bed slope, h is the hydraulic radius (approximated by mean flow depth), and τ_b (N m^{-2}) is the bed shear stress.

[35] In addition to the bed load, the coarse fraction also contains the portion of the suspendible bed material that cannot access the floodplain. This component is defined in Figure 8b as the medium sand traveling below the height of the lowest banks in the study reach (LBH), or 0.2 m. Medium sand in the lowest 20 cm was sampled in both the suspended sediment sampler (DH-48) and bed load sampler (Helley-Smith). However, only the data from the Helley-Smith samples were used to compute the medium sand flux below LBH; the data from the DH-48 sampler are used later to compute the flux of medium sand counted with the fine fraction. In order to account for the unsampled layer between LBH and the top of the Helley-Smith sampler (which only samples the lowest 7.5 cm), we used the Rouse concentration profile and a logarithmic water velocity profile to convert fluxes to concentrations. These data are plotted against dimensionless shear stress in Figure 9b and are approximated with the model

$$q_{ms,\text{coarse}} = 0.02\tau_*^{1.9}, \tag{4}$$

where $q_{ms,\text{coarse}}$ is the instantaneous flux of medium sand below LBH per unit channel width. The instantaneous flux of the coarse fraction per meter channel width is the sum of equations (2) and (4).

5.1.2. Fine Fraction

[36] The fine fraction of the sediment load, as defined in Figure 8, comprises the wash load and the portion of the bed material suspended load that can potentially enter the floodplain (i.e., medium sand traveling above LBH). On the basis of textural data and calculations presented in sections 4.2–4.3, the wash load includes all the fine sand, silt, and clay (particles finer than 0.25 mm diameter). Data from the suspended sediment samples collected at LA 2 E show that wash load (fine sand, silt, and clay) concentration is proportional to the 0.4 power of discharge (Figure 10a) but that concentrations are almost an order of magnitude higher near the flood bore (solid circles) than during flow recession (open circles). The hysteresis in the wash load data can be approximated with the following model:

$$C_{wl,\text{rising}} = 21,000Q_p^{0.4} \quad \text{for } t \le t_p, \tag{5a}$$

$$C_{wl,\text{falling}} = 2,500Q_{\text{inst}}^{0.4}, \quad \text{for } t > t_p, \tag{5b}$$

where $C_{wl,\text{rising}}$ and $C_{wl,\text{falling}}$ are the average sediment concentration of fine sediment on the rising and falling limbs of the hydrograph (mg L^{-1}), Q_p is peak discharge (m^3 s^{-1}), Q_{inst} is instantaneous discharge (m^3 s^{-1}), t is time after the passage of the flood bore, and t_p is the time of the first major flood peak. Because discharge typically increases rapidly during the first few minutes of flow, it was impossible to estimate instantaneous discharge for samples collected from the rising limb. The rising limb samples in Figure 10a are plotted against peak discharge because peak discharge serves as an index of the magnitude of the rainstorm (which partly influences sediment concentration near the flood bore). The falling limb samples are plotted

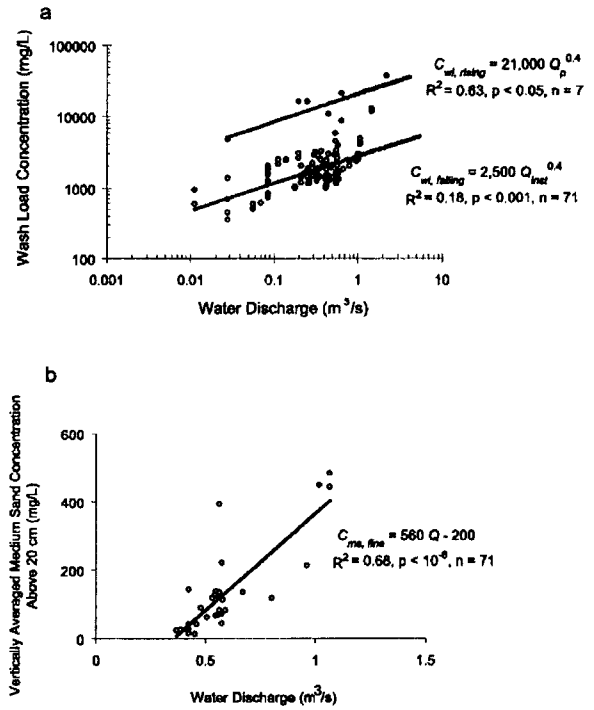

Figure 10. Instantaneous transport rates of the fine sediment fraction. (a) Wash load, consisting of particles finer than 0.25 mm diameter (fine sand and smaller). For a given discharge, wash load concentrations are nearly an order of magnitude higher before peak discharge than afterward, suggesting that the transport rate is limited by supply and that the supply is greatest near the flood bore. Measured wash load concentrations were adjusted to account for the sediment concentration profile below the sampler intake using the Rouse equation. Coefficients in Figure 10a were adjusted to account for transformation bias using a nonparametric correction factor [*Duan*, 1983]. (b) Suspended bed material load (medium sand) traveling above the height of the lowest banks (20 cm). Concentrations in Figure 10b were computed from depth-integrated samples using the Rouse equation. The instantaneous flux of fine sediment equals the sum of the wash load and the suspended bed material load traveling above the height of the banks (see Figure 8 for a definition sketch).

against instantaneous discharge. The concentrations plotted in Figure 10a were increased to account for the concentration profile below the intake of the depth-integrating sampler. Computed corrections for individual samples using equation (1) varied depending on flow depth and the particle size distribution in the sample, but for simplicity a single average correction of +11% was chosen to adjust for the concentration profile below the sampler intake. The regression coefficients in equation (5) have been adjusted by an additional 7% (rising limb) and 6% (falling limb) to correct for transformation bias using a nonparametric correction factor [*Duan*, 1983].

[37] For each suspended sediment (DH-48) sample for which we had particle size information we computed the

medium sand concentration above LBH by applying an adjustment factor to the measured depth-integrated concentration. The adjustment was the ratio of concentration above LBH to the depth-integrated concentration from 7.5 cm to the surface, computed for each particle size class using equation (1) (Figure 10b). A linear regression was fitted to the data in Figure 10b because the power law regression predicted unreasonably high concentrations for high flows beyond the range of the data. The linear regression

$$C_{ms,\mathrm{fine}} = 560Q_{\mathrm{inst}} - 200 \qquad (6)$$

fit the data at least as well as a power law ($p < 10^{-8}$ for linear regression versus $p < 10^{-7}$ for the power law) and was used to compute the long-term flux of medium sand associated with the fine component of the sediment load. The instantaneous flux of fine sediment was computed by multiplying equations (5) and (6) by an appropriate discharge (total discharge for equation (5) and discharge above LBH for equation (6)).

[38] In summary, we used local field data to develop empirical relationships to predict the instantaneous fluxes of both the coarse and fine fractions of the sediment load. The instantaneous transport rate of the coarse fraction increases with about the square of bed shear stress (equations (3) and (4)). In contrast, the instantaneous concentration of the fine fraction, which is related to sediment supply more than flow strength, is approximated with functions of water discharge and time relative to the hydrograph peak (equations (5) and (6)).

5.2. Synthetic Distribution of Rainfall and Runoff

[39] We analyzed rainfall and runoff data from the network of LANL gauges, supplemented with additional discharge data from calibrated crest stage gauges, staff gauges, and pressure transducers, in ULA Canyon to develop a synthetic long-term probability distribution of runoff hydrographs at the upstream end of the study reach. These analyses are explained in detail by *Malmon* [2002] and are only summarized here.

[40] On the basis of the analysis of 1314 discrete rainstorms measured at 11 recording rain gauges on the Pajarito Plateau, *Malmon* [2002] computed frequency distributions of rainstorm depth, duration, and intensity and the temporal pattern of rainfall during events. These data were used to develop a synthetic population of rainstorms during the June–October period, when nearly all of the flash flood-generating rainstorms occur (Table 1). Each of the rainstorms was converted into a flood volume with the Soil Conservation Service (SCS) curve number equation [*U.S. Soil Conservation Service*, 1972], using curve numbers based on measured hydrographs [*Malmon*, 2002]; each of the flood volumes was converted into a flow hydrograph with the synthetic unit hydrograph method using measured hydrographs, following the procedure outlined by *Dunne and Leopold* [1978, p. 333]. In addition, snowmelt was assumed to occur for 66 days per year at a constant discharge of 0.06 $m^3 s^{-1}$ [*Purtymun et al.*, 1990].

5.3. Long-Term Sediment Flux

[41] The sediment transport relationships in equations (2)–(6) were applied to each of the synthetic hydrographs to approximate the amount of sediment transported during floods of a range of magnitude. Figure 11 is an example of a modeled hydrograph and the corresponding sediment discharge for a flow event triggered by a 25 mm rainstorm (with estimated frequency ~1.5 events yr^{-1}). The event yields were then multiplied by event frequency and summed to estimate the long-term average rates of sediment transport of both the fine and coarse fractions by summer flash floods (Table 1). For the snowmelt hydrograph, only the coarse sediment relationships based on the Helley-Smith samples (equations (2) and (4)) were applied, following the observation that snowmelt runoff can move bed material but does not contain high concentrations of fine sediment.

[42] In addition to the potential measurement errors discussed in section 3, there are a number of potential sources of error involved in this extrapolation to estimate long-term fluxes. First, the flux estimates in Table 1 are based on extrapolation of our empirically derived equations to discharges much larger than those we sampled. This extrapolation is necessary because we were not able to sample very large floods, but it is probably reasonable because there is no field evidence that different erosional processes (such as landslides) operate during such events. Second, we applied the empirical transport relationships for the coarse fraction, which were based on data from flash floods, to snowmelt runoff. Coarse sediment transport by snowmelt may be influenced by factors not present during storm runoff (such as higher water viscosities caused by lower water temperatures), so applying the same shear-based relationship derived from measurements of storm flow may have led to some error in our estimate of the snowmelt load. Third, while our approximation of the hypothetical distribution of flow events was based on the best available rainfall and runoff data, our characterization of the long-term climatic and runoff characteristics of the field area may also include errors. Owing to the potential sources of error inherent in extrapolating our data, our estimates of the long-term fluxes in Table 1 are considered approximations.

[43] The long-term average sediment yield below the DP-ULA Canyon confluence was computed to be 2200 t yr^{-1}, consisting of ~50% fine sediment and 50% coarse sediment (Table 1). About 65% (700 t) of the 1100 t of coarse sediment is transported by flash floods; the remaining 400 t moves during snowmelt runoff.

5.4. Frequency and Magnitude of Contributions to the Long-Term Sediment Flux

[44] *Wolman and Miller* [1960] suggested that sediment transport processes can often be expressed by power functions of discharge, the frequency distributions of which are often lognormal. Therefore, they argued, measures of the geomorphic effectiveness of events of different magnitudes and frequencies should have a maximum. This maximum indicates the recurrence interval of the event that transports the most sediment, which they called the effective discharge. They analyzed records from numerous rivers in the United States and concluded that the greatest portion of the sediment load of these rivers is carried by flows with recurrence intervals of less than 1 year. *Nash* [1994] reexamined the magnitude-frequency analysis using a more extensive data set and showed that the recurrence interval of the effective discharge varied widely, ranging from days to

Table 1. Sediment Discharge From Upper Los Alamos Canyon

	Rainfall Depth,[c] mm	Event Frequency,[d] number per year	Modeled Peak Discharge, m^3 s	Sediment Discharge Per Event[a]		Average Annual Sediment Discharge[b]	
				Fine Sediment, t $event^{-1}$	Coarse Sediment, t $event^{-1}$	Fine Sediment, t $event^{-1}$	Coarse Sediment, t $event^{-1}$
	5	3	1	10	10	30	30
	10	5	2	30	20	130	110
	15	4	3	50	40	190	140
	20	3	4	70	50	190	120
	25	2	5	100	60	160	90
	30	0.8	6	150	80	130	70
	35	0.4	7	220	110	100	50
	40	0.2	9	310	130	70	30
	45	0.1	11	430	170	50	20
	50	0.06	12	580	210	30	10
	55	0.03	14	770	250	20	7
	60	0.01	16	1000	290	10	4
	65	0.01	19	1300	340	8	2
	70	0.003	21	1600	390	5	1
	75	0.001	23	2000	450	3	1
	80	0.001	26	2400	500	2	0
	85	0.0003	28	2800	560	1	0
Annual totals from storm runoff						1100	700
Average annual discharge during snowmelt runoff							400
Computed long-term sediment discharge, t yr^{-1}						**1100**	**1100**

[a]Event-integrated sediment discharge computed by applying sediment rating curves (equations (2)–(6) in text) to synthetic hydrographs (see Figure 11 for an example).
[b]Event sediment discharge times event frequency.
[c]Only storms 5 mm and larger were included in frequency estimates as smaller events do not produce appreciable runoff.
[d]Frequency is for 5 mm bins (e.g., 7.5–12.5 mm), except for the first bin (5–7.5 mm rainstorm depth).

decades. This variability is controlled by climatic, drainage basin, and river valley characteristics. *Dunne* [1979], for example, showed that this effective discharge measure varied with land cover for rivers in Kenya.

[45] Despite the fact that sediment supply and rapid flow fluctuation exert first-order controls on sediment transport during individual events, the *Wolman and Miller* [1960] generalization appears to apply to small streams on the Pajarito Plateau. Using peak discharge as a measure of event magnitude, Figure 12 shows that the sediment yield per event can be expressed as a power function of flood size. The total discharge of fine sediment per event increases with peak discharge to the 1.7 power (due mainly to increasing runoff volume), and the total discharge of coarse sediment increases with the 1.2 power of peak flow (due to increasing shear stress). Over 10^1–10^2 years the estimated sediment flux in ULA Canyon is dominated by frequent events, and the contribution of large, rare events appears to be smaller (Figure 13). More than 70% of the annual sediment flux from ULA Canyon over several decades is contributed by events which occur at least once per year (including snowmelt runoff (Table 1)). The most effective storm flows for transporting both fine and coarse sediment are generated by rainstorms between 10 and 30 mm, which occur several times per year (Figure 13). Approximately 70% of the total sediment load is transported by flows that occur, on average, more than once per year. Flows generated by rainstorms with recurrence intervals greater than 10 years contribute only 5% to the estimated long-term sediment yield from ULA Canyon (Table 1). While these estimates may be partially influenced by urbanization in the watershed, frequent flooding (multiple events per year) has also been observed in many nonurbanized watersheds on the Pajarito Plateau [e.g., *Shaull et al.*, 2003]. Because frequent, moderate events transport most of the sediment, such events are also dominant with respect to floodplain formation. Using the relationships in Figures 9 and 10 and a simple floodplain sedimentation model, *Malmon* [2002] computed that most of the vertical accretion in ULA Canyon is accomplished by events that occur more than once every 2 years: floods large enough to flow over bank, yet small enough that a high percentage of the fine sediment that

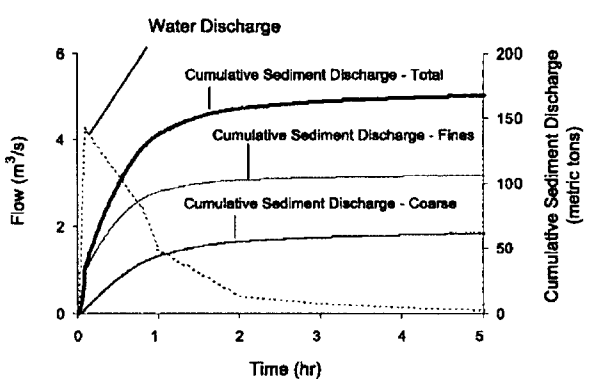

Figure 11. Modeled hydrograph and associated sediment discharge for a flash flood generated by a 25 mm rainstorm. Rainstorms of this magnitude occur ~1.5 times per year at a given location on the Pajarito Plateau [*Malmon*, 2002].

enters the floodplain deposits there before reentering the main channel.

6. Discussion and Conclusions

[46] The purpose of this paper was to investigate how flash floods sort the sediment load of sand-dominated ephemeral channels. This was done by documenting sediment transport processes in detail for a particular field site, upper Los Alamos Canyon, New Mexico. We found that fluvial processes sort the sediment load into two discrete populations: a coarse fraction that interacts with the channel bed and a fine fraction that interacts with the floodplain. The valley floor is composed of coarse and fine sediment deposits stored near the channel bed and in adjacent floodplains, respectively. The coarse-grained deposits (medium sand and coarser sediment) are texturally similar to the bed material load during flood events, and the average texture of the fine-grained deposits (medium sand and finer sediment) resembles that of the suspended load.

[47] The concentration of fine sediment in the flow is always highest near the flood bore and decreases rapidly after the flood wave passes. This suggests that the transport rate of fine sediment is controlled by its supply, which is highest during the earliest stages of flow as a result of factors not directly related to the strength of the flow: (1) bank collapse and fine sediment deposition during the waning stages of the previous flow; (2) bioturbation and raveling between events, both on hillsides and along the channel margins; and (3) rainfall and runoff processes on the hillslopes, which occur prior to the arrival of the flood bore. In contrast, coarse sediment is available from the channel bed, so its transport rate is controlled primarily by the strength and duration of the flow.

[48] Over several decades the computed fluxes of the two sediment fractions are approximately equal. However, while fine sediment is transported primarily during storm runoff in the months between June and October, nearly 40% of the coarse sediment fraction is transported during snowmelt runoff in the spring. Over 10^1-10^2 years, each of the components of the sediment discharge is dominated by small to moderate runoff events. More than 70% of the annual sediment flux (including snowmelt runoff) occurs during events with expected frequencies of more than once

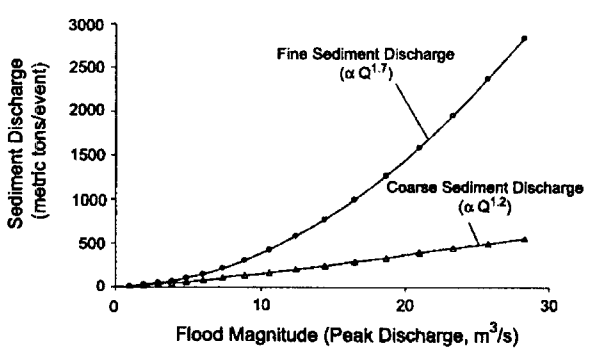

Figure 12. Total event sediment yields, computed by integrating equations (2)–(6) over synthetic hydrographs and plotted against peak discharge.

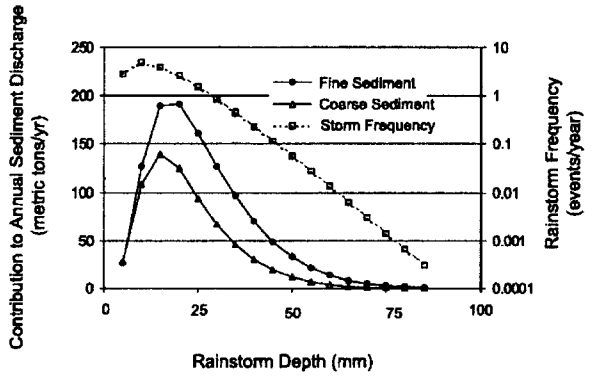

Figure 13. Contributions of rainstorms of varying magnitude and frequency to the computed average annual sediment load in ULA Canyon. Snowmelt runoff transports an additional 400 t yr^{-1} of coarse sediment that is not represented in this plot.

per year. While fluxes per event increase with flow magnitude, over the long term the large number of small flows accomplishes most of the transport. Less than 5% of the computed sediment transport occurs during events with recurrence intervals greater than 10 years.

[49] The mechanisms by which sediment is transported and sorted by flash floods determine the composition of both the bed and the banks, the rates and timing of floodplain construction and overturn, and long-term cycles of aggradation and degradation in semiarid valleys. In our study area, flash floods partition the sediment load into two distinct populations that are supplied by different sources, transported by different mechanisms, and stored in distinct sediment storage reservoirs within the valley floor, for characteristic timescales. This type of partitioning is likely to occur in many sand-dominated ephemeral channels and can be an important mechanism influencing the geomorphology and sedimentology of semiarid valleys.

[50] **Acknowledgments.** This work was supported by the U.S. Department of Energy through a Cooperative University Los Alamos Research (CULAR) grant, by the LANL Environmental Restoration Project, and by a Horton Research Grant from the American Geophysical Union. The authors thank Al Pratt for support during this work, Steve Pearson and Celina Salazar for field assistance, and David Shaull for hydrologic data. We thank Robert Anderson, Manny Gabet, Danny Katzman, David Topping, Pat Wiberg, and an anonymous reviewer for helpful review comments. Los Alamos National Laboratory report LA-UR-03-4521.

References

Babcock, H. M., and E. M. Cushing (1941), Recharge to ground water from floods in a typical desert wash, Pinal County, Arizona, *Eos Trans. AGU*, *23*, 49–56.

Beverage, J. P., and J. K. Culbertson (1964), Hyperconcentrations of suspended sediment, *J. Hydraul. Div. Am. Soc. Civ. Eng.*, *90*, 117–128.

Bowen, B. M. (1990), Los Alamos climatology, *Rep. LA-1,735-MS*, 254 pp., Los Alamos Natl. Lab., Los Alamos, N. M.

Burkham, D. E. (1970), Depletion of streamflow by infiltration in the main channels of the Tucson Basin, southeastern Arizona, *U.S. Geol. Surv. Water Supply Pap., 1939-B*, 36 pp.

Burned Area Emergency Rehabiliatation Team (2000), Cerro Grande fire—Burned area rehabilitation plan, Los Alamos, N. M.

Cannon, S. H., E. R. Bigio, and E. Mine (2001), A process for fire-related debris flow initiation, Cerro Grande fire, New Mexico, *Hydrol. Processes*, *15*, 3011–3023.

Dale, M. R. (1996), Preliminary assessment of radionuclide transport via storm-water runoff in Los Alamos Canyon, New Mexico, *Field Conf. Guideb. N. M. Geol. Soc.*, *47*, 469–472.

Dietrich, W. E. (1982), Settling velocity of natural particles, *Water Resour. Res.*, *18*, 1615–1626.

Duan, N. (1983), Smearing estimate: A nonparametric retransformation method, *J. Am. Stat. Assoc.*, *78*, 605–610.

Dunkerley, D., and K. Brown (1999), Flow behaviour, suspended sediment transport and transmission losses in a small (sub-bank-full) flow event in an Australian desert stream, *Hydrol. Processes*, *13*, 1577–1588.

Dunne, T. (1979), Sediment yield and land use in tropical catchments, *J. Hydrol.*, *42*, 281–300.

Dunne, T., and L. B. Leopold (1978), *Water in Environmental Planning*, 818 pp., W. H. Freeman, New York.

Frostick, L. E., I. Reid, and J. T. Layman (1983), Changing size distribution of suspended sediment in arid-zone flash floods, *Spec. Publ. Int. Assoc. Sedimentol.*, *6*, 97–106.

Gerson, R. (1977), Sediment transport for desert watersheds in erodible materials, *Earth Surf. Processes*, *2*, 343–361.

Graf, W. L. (1987), *Fluvial Processes in Dryland Rivers*, 346 pp., Springer-Verlag, New York.

Graf, W. L. (1994), *Plutonium in the Rio Grande: Environmental Change and Contamination in the Nuclear Age*, 329 pp., Oxford Univ. Press, New York.

Graf, W. L. (1996), Transport and deposition of plutonium-contaminated sediments by fluvial processes, Los Alamos Canyon, New Mexico, *Geol. Soc. Am. Bull.*, *108*, 1342–1355.

Harrelson, C. C., C. L. Rawlins, and J. P. Potyondy (1994), Stream channel reference sites: An illustrated guide to field technique, *Gen. Tech. Rep. RM-245*, 61 pp., U.S. Dept. of Agric. For. Serv., Fort Collins, Colo.

Helley, E. J., and W. Smith (1971), Development and calibration of a pressure-difference bedload sampler, *U.S. Geol. Surv. Open File Rep.*, *8037-01*, 18 pp.

Johansen, M., T. E. Hakonson, and D. D. Breshears (2001), Post-fire runoff and erosion from rainfall simulation: Contrasting forest with shrublands and grasslands, *Hydrol. Processes*, *15*, 2953–2965.

Katzman, D., R. T. Ryti, M. Tardiff, and B. Hardesty (1999), Evaluation of sediment and alluvial groundwater in DP Canyon, *Rep. LA-UR-99-4238*, Los Alamos Natl. Lab., Los Alamos, N. M.

Laronne, J. B., and I. Reid (1993), Very high bedload sediment transport in desert ephemeral rivers, *Nature*, *366*, 148–150.

Lavine, A., D. Katzman, S. L. Reneau, G. A. Kuyumjian, and D. V. Malmon (2001), The Los Alamos Reservoir: A gauge for increased erosion after the Cerro Grande fire, Los Alamos, New Mexico, *Eos Trans. AGU*, *82*(47), Fall Meet. Suppl., Abstract H52B-0421.

Lekach, J., and A. P. Schick (1982), Suspended sediment in desert floods in small catchments, *Isr. J. Earth Sci.*, *31*, 144–156.

Leopold, L. B., and J. P. Miller (1956), Ephemeral streams—Hydraulic factors and their relation to the drainage net, *U.S. Geol. Surv. Prof. Pap.*, *282-A*, 37 pp.

Leopold, L. B., M. G. Wolman, and J. P. Miller (1964), *Fluvial Processes in Geomorphology*, 522 pp., W. H. Freeman, New York.

Leopold, L. B., W. W. Emmett, and R. M. Myrick (1966), Channel and hillslope processes in a semiarid area, New Mexico, *U.S. Geol. Surv. Prof. Pap.*, *352-G*, 193–253.

Levinson, A. A. (1980), *Introduction to Exploration Geochemistry*, 2nd ed., 924 pp., Appl. Pub., Wilmette, Ill.

Malmon, D. V. (2002), Sediment trajectories through a semiarid valley, Ph.D. diss., 334 pp., Univ. of Calif., Santa Barbara.

Malmon, D. V., D. Katzman, A. Lavine, J. E. Lyman, and S. L. Reneau (2002), Sediment budget for a small canyon downstream of the Cerro Grande wildfire, New Mexico, *Geol. Soc. Am. Abstr. Programs*, *34*(7), 471.

Malmon, D. V., T. Dunne, and S. L. Reneau (2003), Stochastic theory of particle trajectories in alluvial valley floors, *J. Geol.*, *111*, 525–542.

Martin-Vide, J. P., D. Ninerola, A. Bateman, A. Navarro, and E. Velasco (1999), Runoff and sediment transport in a torrential ephemeral stream of the Mediterranean coast, *J. Hydrol.*, *225*, 118–129.

McLean, S. R. (1991), Depth-integrated suspended-load calculations, *J. Hydraul. Eng.*, *117*, 1440–1458.

Moody, J. A., and D. A. Martin (2001), Post-fire, rainfall intensity-peak discharge relations for three mountainous watersheds in the western USA, *Hydrol. Processes*, *15*, 2981–2993.

Nash, D. B. (1994), Effective sediment-transporting discharge from magnitude-frequency analysis, *J. Geol.*, *102*, 79–95.

Newman, B. D., A. R. Campbell, and B. P. Wilcox (1998), Lateral subsurface flow pathways in a semiarid ponderosa pine hillslope, *Water Resour. Res.*, *34*, 3485–3496.

Nyhan, J. W., L. W. Hacker, T. E. Calhoun, and D. L. Young (1978), Soil survey of Los Alamos County, New Mexico, *Rep. LA-6779-MS*, Los Alamos Sci. Lab., Los Alamos, N. M.

Purtymun, W. D., G. L. Johnson, and E. C. John (1966), Distribution of radioactivity in the alluvium of a disposal area at Los Alamos, N. M., *U.S. Geol. Surv. Prof. Pap.*, *550-D*, 267 pp.

Purtymun, W. D., R. Peters, and M. N. Maes (1990), Transport of plutonium in snowmelt run-off, *Lab. Rep. LA-1,795-MS*, Los Alamos Natl. Lab., Los Alamos, N. M.

Reid, I., and L. E. Frostick (1987), Flow dynamics and suspended sediment properties in arid zone flash floods, *Hydrol. Processes*, *1*, 239–253.

Reid, I., and J. B. Laronne (1995), Bed load sediment transport in an ephemeral stream and a comparison with seasonal and perennial counterparts, *Water Resour. Res.*, *31*, 773–781.

Reid, I., J. B. Laronne, and D. M. Powell (1998), Flash-flood and bedload dynamics of desert gravel-bed streams, *Hydrol. Processes*, *12*, 543–557.

Renard, K. G., and E. M. Laursen (1975), Dynamic behavioral model of ephemeral stream, *J. Hydraul. Div. Am. Soc. Civ. Eng.*, *92*, 511–528.

Reneau, S. L., and E. V. McDonald (1996), Landscape history and processes on the Pajarito Plateau, northern New Mexico, *Rep. LA-UR-3035*, 179 pp., Los Alamos Natl. Lab., Los Alamos, N. M.

Reneau, S. L., R. T. Ryti, M. Tardiff, and J. Linn (1998), Evaluation of sediment contamination in Upper Los Alamos Canyon (reaches LA-1, LA-2, and LA-3), *Rep. LA-UR-98-3974*, Los Alamos Natl. Lab., Los Alamos, N. M.

Rouse, H. (1937), Modern conceptions of mechanics of fluid turbulence, *Trans. Am. Soc. Civ. Eng.*, *102*, 463–505.

Salomons, W., and U. Forstner (1984), *Metals in the Hydrocycle*, 349 pp., Springer-Verlag, New York.

Schick, A. P., J. Lekach, and M. A. Hassan (1987), Bed load transport in desert floods: Observations in the Negev, in *Sediment Transport in Gravel-Bed Rivers*, edited by C. R. Thorne et al., pp. 617–637, John Wiley, Hoboken, N. J.

Schumm, S. A., and R. F. Hadley (1957), Arroyos and the semiarid cycle of erosion, *Am. J. Sci.*, *255*, 161–174.

Sharma, K. D., N. S. Vangani, and J. S. Chaudhari (1984), Sediment transport characteristics of the desert streams in India, *J. Hydrol.*, *67*, 261–272.

Shaull, D. A., D. Ortiz, M. R. Alexander, and R. P. Romero (2003), Surface water data at Los Alamos National Laboratory, 2002 water year, *Rep. LA-14,019-PR*, 102 pp., Los Alamos Natl. Lab., Los Alamos, N. M.

Smith, R. L., R. A. Bailey, and C. S. Ross (1970), Geologic map of the Jemez Mountains, New Mexico, *U.S. Geol. Surv. Misc. Geol. Invest. Map, I-571*.

Stone, G., and D. Holt (1996), Meteorological monitoring at Los Alamos, *Rep. LA-UR-95-3697*, Los Alamos Natl. Lab., Los Alamos, N. M.

Sutherland, R. A., and R. B. Bryan (1989), Flow dynamics and the variability of suspended sediment in a semiarid tropical stream, Baringo District, Kenya, *Geogr. Ann.*, *72A*, 23–39.

U.S. Soil Conservation Service (1972), *SCS National Engineering Handbook, Section 4: Hydrology*, U.S. Dept. of Agric., Washington, D. C.

Wilcox, B. P. (1994), Runoff and erosion in intercanopy zones of pinyon-juniper woodlands, *J. Range Manage.*, *47*, 285–295.

Wilcox, B. P., B. D. Newman, D. Brandes, D. W. Davenport, and K. Reid (1997), Runoff from a semiarid ponderosa pine hillslope in New Mexico, *Water Resour. Res.*, *33*, 2301–2314.

Wilson, C. J., J. W. Carey, P. C. Beeson, M. O. Gard, and L. J. Lane (2001), A GIS-based hillslope erosion and sediment delivery model and its application in the Cerro Grande burn area, *Hydrol. Processes*, *15*, 2995–3010.

Wolman, M. G., and J. P. Miller (1960), Magnitude and frequency of forces in geomorphic processes, *J. Geol.*, *68*, 54–74.

T. Dunne, Donald Bren School of Environmental Science and Management, 2400 Bren Hall, University of California, Santa Barbara, CA 93106-5131, USA. (tdunne@bren.ucsb.edu)

D. V. Malmon, Department of Geological Sciences, University of California, Santa Barbara, CA 93106, USA. (malmon@bren.ucsb.edu)

S. L. Reneau, Environmental Geology and Spatial Analysis Group, Los Alamos National Laboratory, Los Alamos, NM 87545, USA. (sreneau@lanl.gov)